Photon polarisation in electron-seeded pair-creation cascades

B. King,* N. Elkina,† and H. Ruhl‡

Ludwig-Maximilians-Universität München,

Theresienstraße 37, 80333 München, Germany

(Dated: January 30, 2013)

Abstract

An electromagnetic pair-creation cascade seeded by an electron or a photon in an intense plane wave interacts in a complicated way with the external field. Many simulations neglect the vector nature of photons by including their interaction using unpolarised cross-sections. After deriving rates for the tree-level processes of non-linear Compton scattering and pair creation with an arbitrary linearly-polarised photon in a constant-crossed field, we present results of numerical simulations that include the photon's vector nature. The simulations of seed electrons in a rotating electric field of optical frequency on the one hand support the approximation of using unpolarised cross-sections for tree-level processes to within around 5%, whereas on the other, indicate after $1/2\pi$ periods, more than a factor 3 difference in the distribution of photon polarisations and more than a 40% difference in the number of pairs created by these polarisations. Moreover, these figures were seen to increase with simulation time. The results are particularly of relevance when the external field is anisotropic and the polarisation of the photon is influenced by its environment.

PACS numbers: 52.27.Ep, 13.88.+e

* ben.king@physik.uni-muenchen.de

† nina.elkina@physik.uni-muenchen.de

‡ hartmut.ruhl@physik.uni-muenchen.de

I. INTRODUCTION

There are many examples of macroscopic phenomena originating from a repeated series of microscopic events. One prominent example is the process of nuclear fission, where a seed neutron collides with a ^{235}U nucleus, releasing ^{92}Kr, ^{141}Ba daughter nuclei, gamma-photons and other high-energy neutrons that can further propagate a chain reaction [1]. Another is so-called "particle showers", often used by calorimeters for detection in particle physics, where an incident high-energy particle is brought to radiate, e.g. by passing through matter, and the radiation liberates other particles which in turn can radiate and further propagate the shower [2, 3]. This can occur irrespective of whether the seed particle is charged, such as in the common case of electrons, or whether it is neutral in the case of photons. In such examples, it is typically a safe assumption that in the time between radiating or freeing other particles, the seed particles propagate in a simple way [4]. In contrast, the cascades of pair-creation and Compton-scattering events initiated in intense electromagnetic fields that can lead to the generation of electron-positron plasmas have a much more complicated development. From the moment the initial particles are created, using seeds or directly from vacuum, their exponential growth and recycling of the external field through absorption and re-emission can lead to a complicated interplay between the driving external field and the driven plasma, with such systems predicted to occur, for example when intense electromagnetic fields irradiate single or collections of particles [5, 6], for example in solids [7]. Although electron-seeded pair creation has been demonstrated experimentally [8], profuse positron creation with lasers has thus far been mainly demonstrated via the Bethe-Heitler process of pair-creation by a high-energy photon in the Coulomb field of a nucleus [4, 9].

In order to better understand such systems, there has been an intensification of research efforts to simulate such plasmas [5–7]. Due to their complexity, to model a large number of particles, many approximations have to be made. The purpose of this paper is to investigate one such approximation, namely that the polarisation of photons propagating the cascade can be effectively neglected, being set to the average polarisation angle. To achieve this, we also present a derivation of the linearly-polarised Compton-scattering cross-section in a constant crossed field, which we were unable to find anywhere else in the literature, although the unpolarised cross-section and pair-creation cross-section for definite polarisation

have been derived some time ago [10, 11]. Most recently, arbitrary photon polarisation has been studied in relation to tree-level Compton scattering [12] and pair-creation [13] in finite laser pulses (a review of strong-field QED effects can be found in [14–17]). One instance where photon polarisation in relativistic plasmas is expected to play a role is in the strong magnetic field of certain astrophysical objects such as magnetars [18, 19].

In the current paper, we present calculations performed for a constant-crossed-field background as this is a good approximation when the formation lengths of processes are much smaller than inhomogeneities in the field. More precisely, any arbitrary, time-dependent background can be considered constant on the QED spacetime scale when $\xi = (e^2 p_\mu T^{\mu\nu} p_\nu)/(m^2(\varkappa p)^2) \ll 1$, (using the definition of ξ derived in [20]) where $T^{\mu\nu}$ is the energy-momentum tensor, $\varkappa$ is the external-field wavevector, p is the momentum of particle involved, $e > 0$ and m are the charge and rest-energy of a positron respectively and we work in a system of units in which $\hbar = c = 1$. In terms of laser fields, ξ is often referred to as the "intensity" or "classical non-linearity" parameter, $\xi = m\chi_0/\omega$, $\chi_0 = E_0/E_{\rm cr}$, E_0 is the electric field amplitude and $E_{\rm cr} = m^2/e$ is the critical, so-called "Schwinger" field. Moreover, an arbitrary, constant field can then be expressed in terms of three relativistic invariants:

$$\chi = \frac{e\sqrt{|p_\mu F^{\mu\nu}|^2}}{m^3}; \quad \mathcal{F} = \frac{e^2 F_{\mu\nu}F^{\mu\nu}}{4m^4}; \quad \mathcal{G} = \frac{e^2 F^*_{\mu\nu}F^{\mu\nu}}{4m^4}, \tag{1}$$

where F and F^* are the electromagnetic tensor and its dual. Any function of these three parameters $W(\chi, \mathcal{F}, \mathcal{G})$ can be considered $\approx W(\chi, 0, 0)$, when $\mathcal{F}, \mathcal{G} \ll \chi^2, 1$. Such functions then describe processes in "crossed" fields ($\mathbf{E}\cdot\mathbf{B} = E^2 - B^2 = 0$, for electric and magnetic field $\mathbf{E}$, $\mathbf{B}$, equivalently $F^2 = F^*F = 0$). At least for laser systems, since $E/E_{\rm cr} \ll 1$, the second of these inequalities is easily fulfilled and as the processes in question only become probable when $\chi \gtrsim 1$, the first inequality will also be fulfilled in the current study. A pedagogical description of constant crossed field Compton scattering has recently been given in [21].

The paper is organised as follows. In Sec. II we present the derivation of Compton-scattering of a polarised photon in a constant-crossed field, discuss the result, then present in Sec. III the rate for creation of pairs due to an arbitrarily linearly-polarised photon, which is fol-

lowed in Sec. IV by a study of these two processes combined – the smallest chain of events considered involving a real photon that can lead to e^--seeded pair creation, and finally the conclusions of the theoretical sections are investigated in Sec. V where results are presented from simulations of chains of lowest-order processes to compare the effect of including polarisation in pair-creation cascades.

II. DERIVATION OF LINEARLY-POLARISED COMPTON SCATTERING RATE IN A CONSTANT CROSSED FIELD

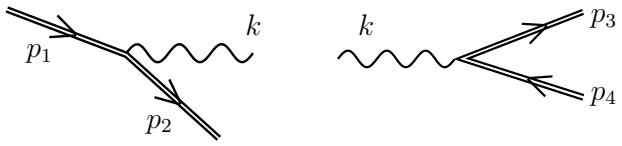

Fig. 1. One example generation in the envisaged cascade, with an on-shell photon linking Compton-scattering (left) and pair-creation (right) processes. Double lines represent dressed wavefunctions that include the interaction with the external field to all orders.

We define a plane wave to be an external field, the vector potential of which is given by $A^\mu = A^\mu(\varphi)$, which is a function solely of the phase $\varphi = \varkappa x$. The solutions to Dirac's equation in such a background field for a particle of momentum p are described by the so-called Volkov wavefunctions [22]:

$$\psi_r(p) = \Big[1 + \frac{e\not{k}\not{A}}{2\varkappa p}\Big]\frac{u_r(p)}{\sqrt{2p^0V}}\mathrm{e}^{iS}; \quad \overline{\psi}_r(p) = \frac{\overline{u}_r(p)}{\sqrt{2p^0V}}\Big[1 + \frac{e\not{A}\not{k}}{2\varkappa p}\Big]\mathrm{e}^{-iS} \tag{2}$$

$$S = -px - \int_{\varphi_0}^{\varphi} d\varphi' \Big(\frac{e(pA(\varphi'))}{\varkappa p} - \frac{e^2A^2(\varphi')}{2(\varkappa p)}\Big), \tag{3}$$

where $u_r(p)$, $\bar{u}_r(p)$ are free-electron spinors, $\not{A} = \gamma^\mu A_\mu$, V is the system volume and where S corresponds to the action from classical electrodynamics of an electron in a plane wave [23]. The limit of a constant crossed field is then achieved by choosing $A^\mu(\varphi) = a^\mu\varphi$ and eventually letting $\varkappa^0 \to 0$ when all dependency on $\varkappa^0$ has disappeared. The amplitude for Compton scattering (the left-hand diagram in Fig. 1) is given by:

$$S_{fi,\gamma} = e\int d^4x\ \overline{\psi}_2(x)\not{\epsilon}\frac{\mathrm{e}^{ikx}}{\sqrt{2k^0V}}\psi_1(x), \tag{4}$$

where k is the momentum of the real photon. Employing the constant-crossed-field limit, choosing $\varphi_0 = 0$, one can write this as:

$$S_{fi,\gamma} = e\int d^4x\ \mathrm{e}^{i(p_2+k-p_1)x}F(\varphi); \qquad F(\varphi) = \mathrm{e}^{i(c_2\varphi^2+c_3\varphi^3)}\frac{\overline{u}_r(p_2)}{\sqrt{2p_2^0V}}\Big[1+\frac{e\not{A}\not{k}}{2\varkappa p_2}\Big]\not{\epsilon}\Big[1+\frac{e\not{\epsilon}\not{A}}{2\varkappa p_1}\Big]\frac{u_r(p_1)}{\sqrt{2p_1^0V}}$$

$$c_2 = -\frac{e}{2}\left(\frac{p_1a}{\varkappa p_1}-\frac{p_2a}{\varkappa p_2}\right); \qquad c_3 = \frac{e^2a^2}{6}\left(\frac{1}{\varkappa p_1}-\frac{1}{\varkappa p_2}\right). \tag{5}$$

By Fourier-transforming $F(\varphi)$ and integrating over x we acquire:

$$S_{fi,\gamma} = (2\pi)^3 e\int dr\ \delta^4(p_2+k-p_1+r\varkappa)\ \Gamma(r); \qquad \Gamma(r) = \int d\varphi\ F(\varphi)\,\mathrm{e}^{-ir\varphi}. \tag{6}$$

To obtain the polarised rate of Compton scattering, R_γ, we use

$$R_\gamma = \frac{V^2}{2T}\int\frac{d^3p_2}{(2\pi)^3}\frac{d^3k}{(2\pi)^3}\ \mathrm{tr}\,|S_{fi,\gamma}|^2, \tag{7}$$

where tr is the trace over spin indices, the factor $1/2$ is due to an average over initial electron spin states and T is the system duration. Using lightfront co-ordinates for momenta $p^{+,-} = (p^0 \pm p^3)/2$, $p^\perp = (p^1, p^2)$ and for co-ordinates $x^{+,-} = x^0 \pm x^3$, $x^\perp = (x^1, x^2)$ and defining at this point the specific co-ordinate system for the calculations with $\varkappa = \varkappa^0(1,0,0,1)$, $a_1 = (0,1,0,0)$ and $a_2 = (0,0,1,0)$, we use the following arguments to deal with the delta-function in Eq. (6):

$$|S_{fi,\gamma}|^2 = (2\pi)^6e^2\int dr\,dr'\ \delta^4(\Delta p+r\varkappa)\delta^4(\Delta p+r'\varkappa)\Gamma(r)\Gamma^\dagger(r') \tag{8}$$

$$|S_{fi,\gamma}|^2 = (2\pi)^6e^2\int dr\,dr'\ \delta^4(\Delta p+r\varkappa)\delta^4[(r'-r)\varkappa]\Gamma(r)\Gamma^\dagger(r') \tag{9}$$

$$|S_{fi,\gamma}|^2 = (2\pi)^6e^2\int dr\,dr'\ \delta^4(\Delta p+r\varkappa)\frac{\delta^4[(r'-r)\varkappa]}{\delta(r-r')}\delta(r-r')\Gamma(r)\Gamma^\dagger(r') \tag{10}$$

$$|S_{fi,\gamma}|^2 = (2\pi)^6e^2\frac{VT}{(2\pi)^3L_{\varphi,\gamma}}\int dr\ \delta^4(\Delta p+r\varkappa)|\Gamma(r)|^2 \tag{11}$$

$$|S_{fi,\gamma}|^2 = (2\pi)^3e^2\frac{VT}{L_{\varphi,\gamma}\varkappa^0}\delta^{(2)}(\Delta p^\perp)\delta(\Delta p^-)|\Gamma(r'_*)|^2, \tag{12}$$

where we have defined: $\Delta p = p_2+k-p_1$ and in the final line integrated over the $^+$ component of the delta-function to give

$$r'_* = \Delta p^+ = \frac{\varkappa^0}{2p_1\varkappa}((p_2+k)^2-m^2) = \varkappa^0\frac{p_2k}{p_1\varkappa}, \tag{13}$$

already using what we will shortly introduce, that all momenta are on-shell, and where we have defined a dimensionless interaction phase length $L_{\varphi,\gamma}$, following standard arguments in e.g. [14]:

$$\delta(r-r')\big|_{r=r'} = \int\frac{dl}{2\pi}\ \mathrm{e}^{i(r-r')l}\Big|_{r=r'} = \frac{L_{\varphi,\gamma}}{2\pi}. \tag{14}$$

By noting that:

$$F_n(r,c_2,c_3) := \int_{-\infty}^{\infty} d\varphi\ (i\varphi)^{n-1} \mathrm{e}^{i(r\varphi+c_2\varphi^2+c_3\varphi^3)}, \tag{15}$$

can be written in terms of the Airy function Ai [24] and its derivative, Ai$'$, where, for example:

$$F_1 = f_1\,\mathrm{Ai}(\nu); \qquad f_1 = \frac{2\pi}{(3c_3)^{1/3}}\mathrm{e}^{i\eta}; \qquad \eta = -\frac{rc_2}{3c_3} + \frac{2c_2^3}{27c_3^2}; \qquad \nu = \frac{r - c_2^2/3c_3}{(3c_3)^{1/3}}, \tag{16}$$

and $F_n = \partial^{n-1} F_1/\partial r^{n-1}$ for $n \in \mathbb{N}_{>0}$, which occur in the definition of $\Gamma(r)$ in Eq. (6), performing the spin trace of $\Gamma(r)$, one arrives at:

$$\begin{aligned} \frac{\mathrm{tr}\,|S_{fi,\gamma}|^2}{VT} &= \frac{(2\pi)^3 e^2 \delta^{(2)}(\Delta p^\perp)\delta(\Delta p^-)}{8p_1^0\,p_2^0\,k^0 L_{\varphi,\gamma}\varkappa^0}\mathrm{tr}\,|\Gamma(r_*)|^2, \\ \mathrm{tr}\,\frac{|\Gamma(r_*)|^2}{8} &= \left|p_1\varepsilon'^*\,F_1 - ie\,a\varepsilon'^*\,F_2\right|^2 + \frac{3c_3}{2}\,\varkappa k\left(|F_2|^2 + \mathrm{Re}\,F_1F_3\right) \end{aligned} \tag{17}$$

where ε' is related to the photon polarisation ε via:

$$\varepsilon'^\mu := \varepsilon^\mu - k^\mu\frac{\varkappa\varepsilon}{\varkappa k} \tag{18}$$

and Eq. (17) agrees with [14] (P. 557, Eq. (36)). The redefinition of ε' in Eq. (18) inspired by [14] is also a valid a polarisation vector, obeying $\varepsilon'^2 = -1$ and $\varepsilon' k = 0$ as required, but is useful in removing higher powers of $k_{x,y}$ from the spin trace. Let us use the following basis for the two polarisation vectors transverse to the photon wavevector (e.g. as used in [25]):

$$\Lambda^\mu_{1,2} = \frac{k\varkappa\ a^\mu_{1,2} - ka_{1,2}\,\varkappa^\mu}{\varkappa k\,\sqrt{-a^2_{1,2}}}, \qquad a_i a_j = -\delta_{ij}\left(\frac{E}{\varkappa_0}\right)^2, \tag{19}$$

where E is the modulus of the electric field, then $\Lambda^\mu_i\Lambda_{j,\mu} = -\delta_{i,j}$ and $\Lambda_i k = 0$ for $i,j, \in \{1,2\}$ as required. When $\varkappa k = 0$ the rate vanishes quicker than $1/\varkappa k$, so the definition in Eq. (19) is sound (see also [21] for an analysis of collinear divergences in Compton scattering). So for a head-on collision of photon and external-field wave-vector, $\Lambda_{1,2} = a_{1,2}$. We seek the rate of scattering for arbitrary linear polarisation. To this end, define the polarisation to be a superposition of these basis vectors

$$\varepsilon^\mu = c_1\Lambda^\mu_1 + c_2\Lambda^\mu_2, \qquad c_1, c_2 \in \mathbb{C}. \tag{20}$$

Since $\varepsilon^2 = -1$, we know $c_2^2 = 1 - c_1^2$. When one combines the expression for the rate R_γ with Eq. (17) and integrates the delta-functions over p_2, just as for the unpolarised cross-section,

the integrand is independent of k_x. However, making the observation (where momenta are now in units of m):

$$\int dk_x = \frac{\chi_0}{\varkappa^0}\frac{\chi_k}{\chi_1}\int d\varphi_*, \tag{21}$$

where φ_* is the saddle-point of the Airy functions in the problem Eq. (15), and one notes that this is the same interaction phase length $L_{\varphi,\gamma}$ defined in Eq. (14), then the integral can be performed, cancelling the $L_{\varphi,\gamma}$ factors. The final manageable integral in k_y is then calculated using:

$$\int_{-\infty}^{\infty} dt\ \mathrm{Ai}^2(t^2+c) = \frac{1}{2}\ \mathrm{Ai}_1(z) := \frac{1}{2}\int_0^{\infty} dt\ \mathrm{Ai}(t+x) \tag{22}$$

$$\int_{-\infty}^{\infty} dt\ \mathrm{Ai}'^2(t^2+c) = -\frac{1}{4\kappa}\left[3\mathrm{Ai}'(z) + c\kappa\mathrm{Ai}_1(z)\right], \tag{23}$$

$$\int_{-\infty}^{\infty} dt\ t^2\mathrm{Ai}^2(t^2+c) = -\frac{1}{4}\ \left[\frac{1}{\kappa}\mathrm{Ai}'(z) + c\,\mathrm{Ai}_1(z)\right] \tag{24}$$

where $z = \kappa c$, $\kappa = 2^{2/3}$, and the derivation of the final integral was based on results from [26]. One then arrives at the rate for Compton scattering for an arbitrarily linearly-polarised photon emitted in a linearly-polarised constant-crossed field:

$$R_\gamma(\phi) = \frac{-\alpha m}{p_1^0}\int_0^{\infty}\frac{dv}{(1+v)^2}\left\{\frac{1}{z}\left[2\cos^2\phi + 1 + \frac{v^2}{1+v^2}\right]\mathrm{Ai}'(z) + \mathrm{Ai}_1(z)\right\}, \tag{25}$$

$$\phi \in [0,\pi[; \qquad z = \mu^{2/3}; \qquad \mu = \frac{\chi_k}{\chi_1(\chi_1-\chi_k)} = \frac{v}{\chi_1}; \qquad \chi_k = \frac{e\sqrt{|F_{\mu\nu}k^\nu|^2}}{m^2} = 2\chi_0 k^-, \tag{26}$$

where we have defined a polarisation angle $c_1 = \cos\phi$, $c_2 = \sin\phi$ ($\phi = 0, \pi/2$ correspond to polarisations $\Lambda_{1,2}$ respectively) and $\alpha = e^2/4\pi$ is the fine-structure constant. As a test of Eq. (25) we note that if one defines $R_{\gamma,0} = [R_\gamma(0) + R_\gamma(\pi/2)]/2$ as the rate of Compton scattering averaged over polarisations, the so-called "unpolarised" rate, then:

$$R_{\gamma,0} = \frac{-\alpha m}{p_1^0}\int_0^{\infty}\frac{dv}{(1+v)^2}\left\{\frac{2}{z}\left[1 + \frac{v^2}{2(1+v^2)}\right]\mathrm{Ai}'(z) + \mathrm{Ai}_1(z)\right\}, \tag{27}$$

which, recalling that momenta are expressed in units of m, agrees with the literature e.g. [14] (P. 559, Eq. (49)).

A. Linearly-polarised Compton scattering rate

In the first plot of Fig. 2, we see how $R_\gamma(\phi)$ depends on the quantum nonlinearity parameter χ as well as the polarisation angle ϕ, where we note the characteristic maximum around

$\chi \approx 1$. We define the relative difference from the unpolarised rate, ΔR_γ thus:

$$\Delta R_\gamma = 2\,\frac{R_\gamma(\phi) - R_{\gamma,0}}{R_\gamma(\phi) + R_{\gamma,0}}, \tag{28}$$

which is plotted in the second plot of Fig. 2. Although the relative difference is largest for small χ_1, we note for the optimum region around $\chi = 1$, there still persists a maximum relative difference of around 50% in the generation of different polarisations.

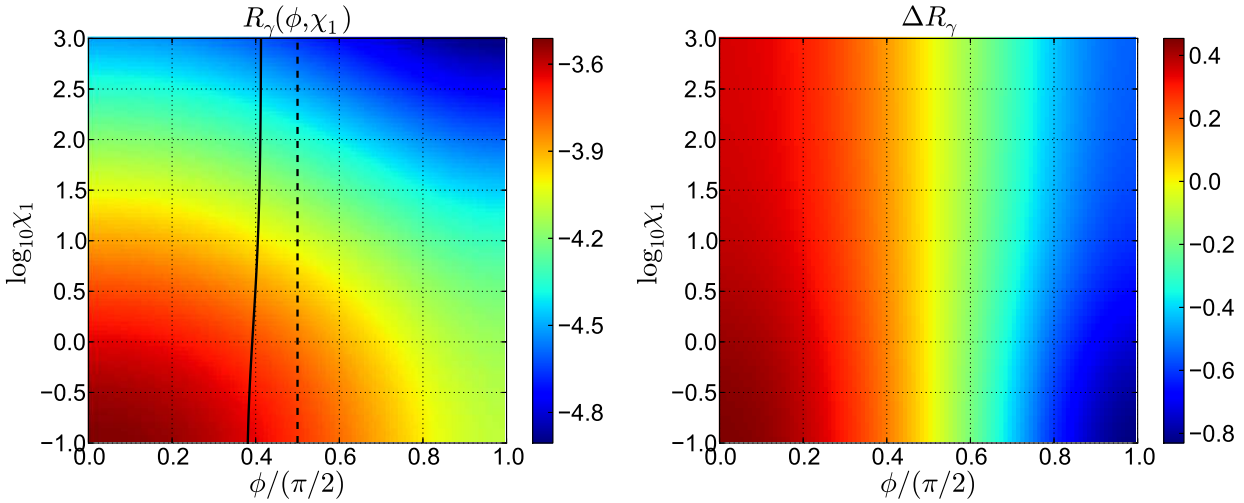

Fig. 2. (Color online). $\Delta R_\gamma = 2(R_\gamma(\phi) - R_{\gamma,0})/(R_\gamma(\phi) + R_{\gamma,0})$, for a head-on collision of electron and external field wave-vector ($\chi_0 = 0.01$). The solid black line indicates the average polarisation produced compared with the unpolarised differential rate (dashed line), which indicates the polarisation of photon that is equivalent to taking the average number produced.

III. POLARISED PAIR CREATION RATE

Pair-creation is a cross-channel of Compton scattering, and the polarised pair-creation rate can be arrived at by making the following substitution in Eq. (17): $p_1 \to -p_4$, $p_2 \to p_3$, $k \to -k$ [23], where the outgoing electron and positron have momenta p_3 and p_4 respectively. By following similar steps to the Compton-scattering derivation, one arrives at:

$$R_e(\phi) = \frac{-\alpha m}{2k^0}\int_1^\infty \frac{du}{u\sqrt{u(u-1)}}\left\{\frac{1}{z}\left[4u - 1 - 2\cos^2\phi\right]\mathrm{Ai}'(z) - \mathrm{Ai}_1(z)\right\}, \tag{29}$$

$$\phi \in [0,\pi[; \qquad z = \mu^{2/3}; \qquad \mu = \frac{\chi_k}{(\chi_k - \chi_3)} = \frac{4u}{\chi_k}; \qquad \chi_3 = \frac{e\sqrt{|F_{\mu\nu}p_1^\nu|^2}}{m^2c^3} = 2\chi_0 p_3^-. \tag{30}$$

This expression can be tested in an even clearer way than $R_\gamma(\phi)$, by comparing $R_e(0)$ and $R_e(\pi/2)$ rates with the known rates for these polarisations, which exactly reproduce the expressions given in e.g. [14]. In Fig. 3 we again plot how the rate depends on χ_k and polarisation angle as well as the relative difference due to this polarisation angle. We note that the optimum rate for pair-creation is at a typically higher value of the quantum non-linearity parameter than for Compton scattering, $\chi_k \approx 10^{1.25}$. Also, we see from the plot of ΔR_e, that photon polarisations which are *more* likely to be produced via non-linear Compton scattering are *less* likely to lead to pair-creation and vice-versa. Due to the different shapes of R_e and R_γ, we will further investigate whether this compensation is seen in a cascade.

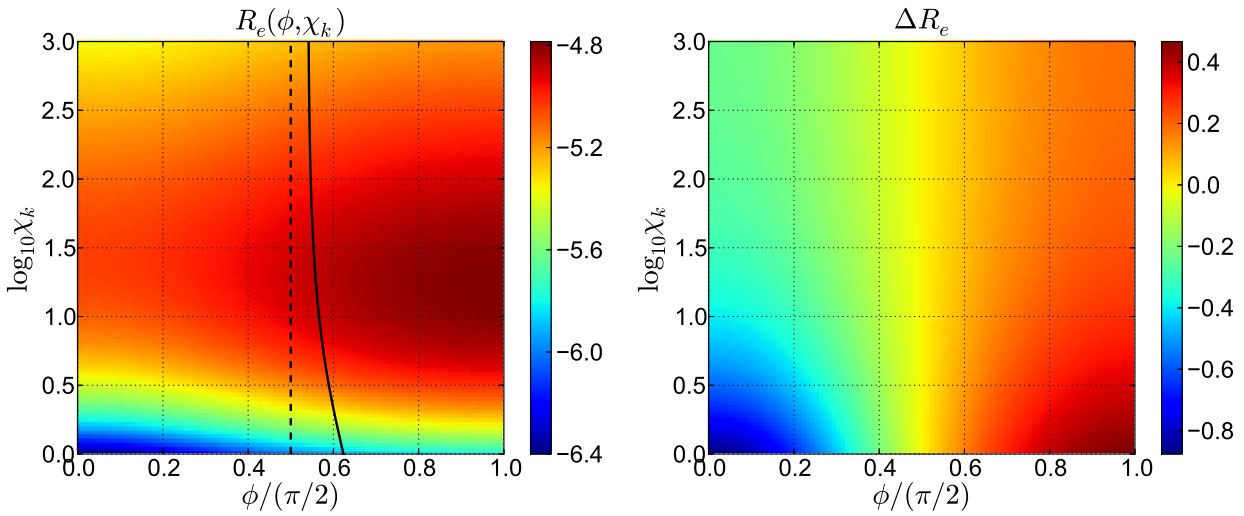

Fig. 3. (Color online). $\Delta R_e = 2(R_e(\phi) - R_{e,0})/(R_e(\phi) + R_{e,0})$ for a head-on collision and $\chi_0 = 0.01$. The solid black line represents the average photon polarisation creating pairs and the dashed line is the photon polarisation that represents the average rate of creating pairs.

IV. EFFECT OF PHOTON POLARISATION ON TWO-STEP FERMION-SEEDED PAIR CREATION

A. Differential rate

Electron- (positron-) seeded pair creation in an external field $e^{-(+)} \rightarrow e^{-(+)} + e^+e^-$ can proceed via a two-step process, where the intermediate photon becomes real and then decays to a pair, or via a one-step process where the intermediate photon remains virtual [27]. Until

now, the only scenario in which the virtual process has been shown to be dominant, to the best of our knowledge, is by tuning the external-field frequency to exploit a resonance in the photon propagator in the multi-photon regime ($\xi \ll 1$) [28]. As the constant crossed field calculation is valid in the limit of zero external-field frequency ($\xi \to \infty$), this effect can be ruled out. Assuming that spin effects of the incoming and outgoing fermions are negligible (including spin-effects originating from radiative corrections to the Volkov states [29]), it is supposed that taking fermion-seeded pair creation in a constant crossed field to be given entirely by the real process, is a good approximation. Let us write this in terms of the expected number of pairs per unit phase required to Compton-scatter $L_{\varphi,\gamma}$ and to pair-create $L_{\varphi,e}$. To do this, we use the relation $mT_j/p_j^0 = L_{\varphi,j}/(\varkappa p_j)$. Then the differential rate (probability per unit interaction phase length) for the two-step process, $R_{\gamma e}(\varphi)$, can be formulated as:

$$R_{\gamma e}(\phi) = \int dv \, \frac{\partial R_\gamma(v,\phi)}{\partial v} \, R_e\left(\chi_k(v),\phi\right) \frac{k^0 p_1^0 \chi_0^2}{\chi_1 \chi_k(v)}, \tag{31}$$

where $\chi_k(v) = \chi_1 v/(1+v)$. One can then plot the differential rate of the electron step for each of the polarisation possibilities, $\partial R_{\gamma e,l}/\partial\chi_3$, where $l = 0$ is the unpolarised rate, $l = 1, 2$ those corresponding to polarisation $\Lambda_{1,2}$ in Eq. (19) and $R_{\gamma e} = \langle R_{\gamma e}(\phi)\rangle_\phi$ (where $\langle\rangle_\phi$ corresponds to taking the average over ϕ), displayed in Fig. 4.

The dynamics for pairs created with differently-polarised photons is very similar, as can be seen by the differential non-linear Compton scattering rates in Fig. 4, although the maxima are slightly displaced and there is a slight asymmetry between $\partial R_{\gamma e}/\partial\chi_3$ and $\partial R_{\gamma e,0}/\partial\chi_3$ as compared to the fixed $l = 1, 2$ polarisations shown by lines crossing in the plots (the plots are identical for $\chi_3 \to \chi_4$ i.e. for electrons and positrons). It can be seen that for a higher incoming χ (χ_1), the proportion of energy given to the created pair becomes, on average, lower, as the distribution in $\chi_3 \in [0, \chi_1[$ becomes increasingly skewed towards the lower end. In fact, χ_3 stays between $0.5 < \chi_3 < 0.75$ for $1 < \chi_1 < 10^3$. This can be explained by noticing that Compton scattering is most probable at $\chi_k \approx 1$ and since $\chi_k = \chi_3 + \chi_4 \approx 2\chi_3$, that the most probable value of χ_3 for $\chi_1 > 1$ (hence allowing $\chi_k > 1$) is around $\chi_3 \approx 0.5$. One could conjecture the existence of the two types of cascade mentioned in the introduction; a *free-particle* and a *field-driven* cascade. For a high-χ incident fermion, it would seem that each Compton-scattering-particle-creation event reduces the χ-factor only slightly. This is

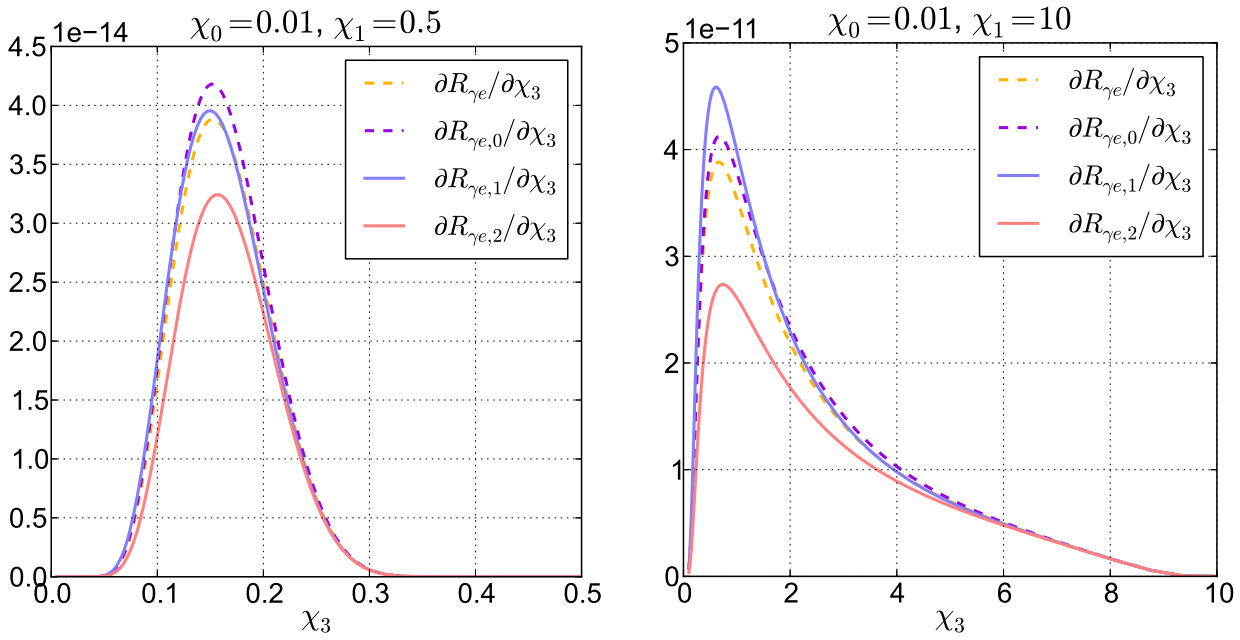

Fig. 4. (Color online). Plot of the differential rate for creating the next generation of pairs, given an incident electron with $\chi_1 = 0.5$ (left) and $\chi_1 = 10$ (right). The solid lines for definite photon polarisation have slightly displaced maxima and as shown in the left-hand plot, do not always denote the maximum and minimum rate.

shown in Fig. 5 where the differential cross-section of $R_{\gamma e}$ in χ_2 (the scattered fermion) is plotted, and the most probable ratio of χ_2/χ_1 is marked with the solid black line. Since the rate $R_{\gamma e}$ is expressed as a probability per unit external-field phase, although large and small values of χ_1 may have the same value of $R_{\gamma e}$, the probability that a pair is created in a given duration in the lab-frame in a homogeneous field is much higher for the higher value of χ as it traverses more external-field phase than the lower-value χ particle. Therefore Fig. 5 shows that if a $\chi_1 \lesssim 5$ fermion produces a pair, further acceleration from the external field will be required before pair-creation becomes comparatively probable again. This would represent a transition from the free-particle to the field-driven cascade. We note that we have focused simply on the two-step pair-creation process, but the two-photon Compton scattering process [30] would most likely be more important to describe the fermion dynamics, as single-photon Compton scattering is more probable than pair-creation for all values of χ considered here.

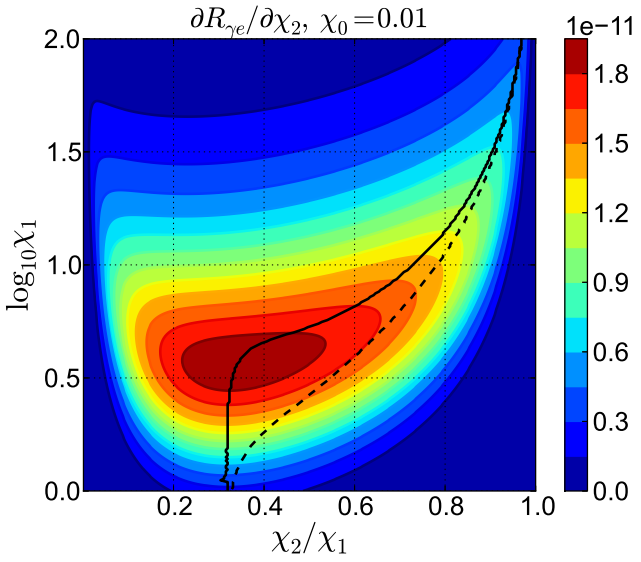

Fig. 5. (Color online). The differential rate of the electron step with respect to the scattered electron. The solid black line marks the most probable χ_2/χ_1 ratio for the scattered electron after emitting a real photon that decays into a pair and the dashed line marks the resulting value (χ_2 becomes χ_1 for the next generation) . The presence of a tail around $\chi_2 = \chi_1$ hints at a cascading process.

B. Total rate

By integrating under the curves in Fig. 4, we acquire an approximation to the fermion two-step rate, $R_{\gamma e}(\phi)$, plotted in Fig. 6. To deduce the overall difference that each polarisation makes, we plot the relative difference, $\Delta[R]$ with respect to $R_{\gamma e}$, $\Delta[R] := (R - R_{\gamma e})/R_{\gamma e}$, displayed in Fig. 6. We notice that although the total rate for photons polarised in the $l = 1, 2$ direction varies with χ_1, the difference between unpolarised $R_{\gamma e,0}$ and polarised $R_{\gamma e}$ rates remains small at approximately 5%, whereas the maximum difference due to polarisation is around a 30% reduction. This represents a smoothing out of the larger relative differences found for the individual processes in Figs. 2, 3. In order to investigate the effect of polarisation when a greater variety of chains of processes occur, we turn to simulation.

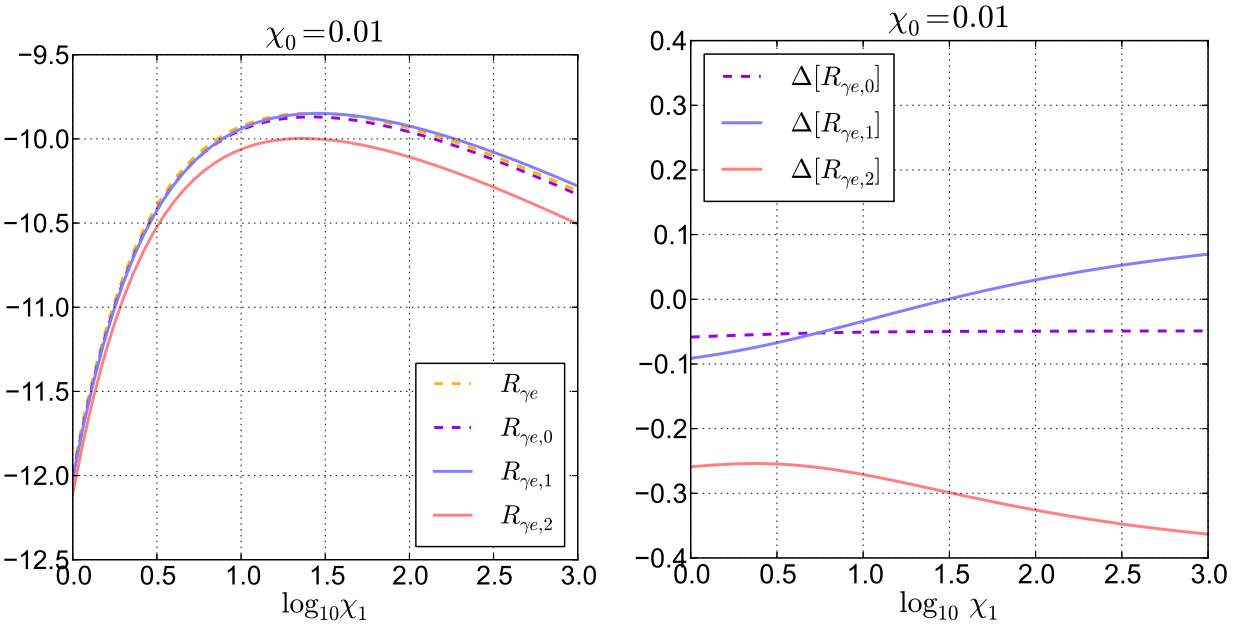

Fig. 6. (Color online). Plot of the total approximation to the two-step process $R_{\gamma e}$ (left) and the relative difference in this approximation from using a polarised intermediate photon $\Delta[R] := (R - R_{\gamma e})/R_{\gamma e}$ (right).

V. CASCADE SIMULATION

We wish to investigate the cumulative effect of photon polarisation when Compton-scattering and pair-creation processes form a cascade. To this end, we employ simulation methods developed in [5, 6], which integrate over these lowest-order rates to approximate chains of events. Simulation has the veritable advantage that all possible chains of real processes are considered, for example that several Compton-scattering steps can occur before a pair-creation step, which for some values of χ_1 have the potential to expose the polarisation behaviour. Moreover, although we have analytically investigated the idealised background of a constant crossed field, in a simulation, one can employ the so-called "locally-constant field approximation," in which the constant crossed field rates are integrated over the phase of a more complicated field. In this case, $\chi \to \chi[E(\varphi)]$, where E is the electric field amplitude with a more complicated structure and φ is its phase. We take the range of validity of such an approximation to be the same as the validity of the constant crossed field expression, already discussed in the paragraph below Eq. (1). However, the higher the variety of chains of events, the more challenging it is to directly compare with theory.

In order to incorporate the polarised cross-sections, we rewrite the rate equations in terms of rates per unit energy $\mathcal{E}$:

$$\frac{dW_\gamma}{d\mathcal{E}_\gamma} = -\frac{\alpha m^2 c^4}{\hbar \mathcal{E}_e^2}\left\{\mathrm{Ai}_1(x) + \left(\frac{2\cos^2\phi + 1}{x} + \chi_k\sqrt{x}\right)\mathrm{Ai}'(x)\right\}, \tag{32}$$

$$\frac{dW_e}{d\mathcal{E}_e} = \frac{\alpha m^2 c^4}{\hbar \mathcal{E}_\gamma^2}\left\{\mathrm{Ai}_1(x) + \left(\frac{2\cos^2\phi + 1}{x} - \chi_k\sqrt{x}\right)\mathrm{Ai}'(x)\right\}, \tag{33}$$

where $x = \mu^{2/3}$, and the expressions resemble those of Eqs. (2,3) in [6]. As an example scenario, we simulate the presence of 10^3 initial electrons in two cases: beginning at rest ($\chi_1(t=0)=0$) and counter-propagating with initial $\chi_1 = 5$ against a rotating electric field $\mathbf{E}(t) = (E_0\cos\varkappa^0 t, E_0\sin\varkappa^0 t, 0)$, where $\varkappa^0 = 1$ eV is the angular frequency and $\xi = 10^4$ ($\chi_0 \approx 0.02$) (the strong-field QED effects in this field are to a good approximation equivalent to those of a constant crossed field background, see also [6]). For each scenario, the four different cases are simulated in which: i) the parameter ϕ is randomly selected from a uniform distribution $\phi \in [0, \pi/2[$ (the more physical case) denoted without an extra subscript; ii) unpolarised rates are used (equivalent to setting $\phi = \pi/4$), denoted by $_{,0}$; iii) $\phi = 0$, denoted by $_{,1}$; iv) $\phi = \pi/2$, denoted by $_{,2}$. The number of fermions with $p^0 > 20$ ($\chi > 0.4(1-\cos\theta)$, where θ is the angle between $\mathbf{p}$ and $\boldsymbol{\varkappa}$) and photons with $\chi_k > 1$ generated with the above parameters are plotted in Figs. 7, 8 respectively. The straight part of the plots represents an equilibrium between momentum change due to QED processes and acceleration by the field. We note that the ratio of photons to fermions is of the order of unity (see Fig. 9), although the number of fermions created by $\varkappa^0 t = 1$ shows that, depending on photon polarisation, the average number of generations in the cascade is between 1.8 and 3.3 (using $N_e = 2(2^n - 1)N_\gamma(t=0)$ as the number of fermions created after n generations).

A. Photon sector

In a plot of the numbers of photons generated in Fig. 7, we make the following observations: i) the production of photons with polarisation $\phi = 0$ is considerably more probable than with $\phi = \pi/2$; ii) the difference in the photons generated using unpolarised and polarised rates is very small (this was also reflected in the frequency spectra) and iii) the time required for photon-production to begin was more than two orders of magnitude larger for the $\chi_1(t =$

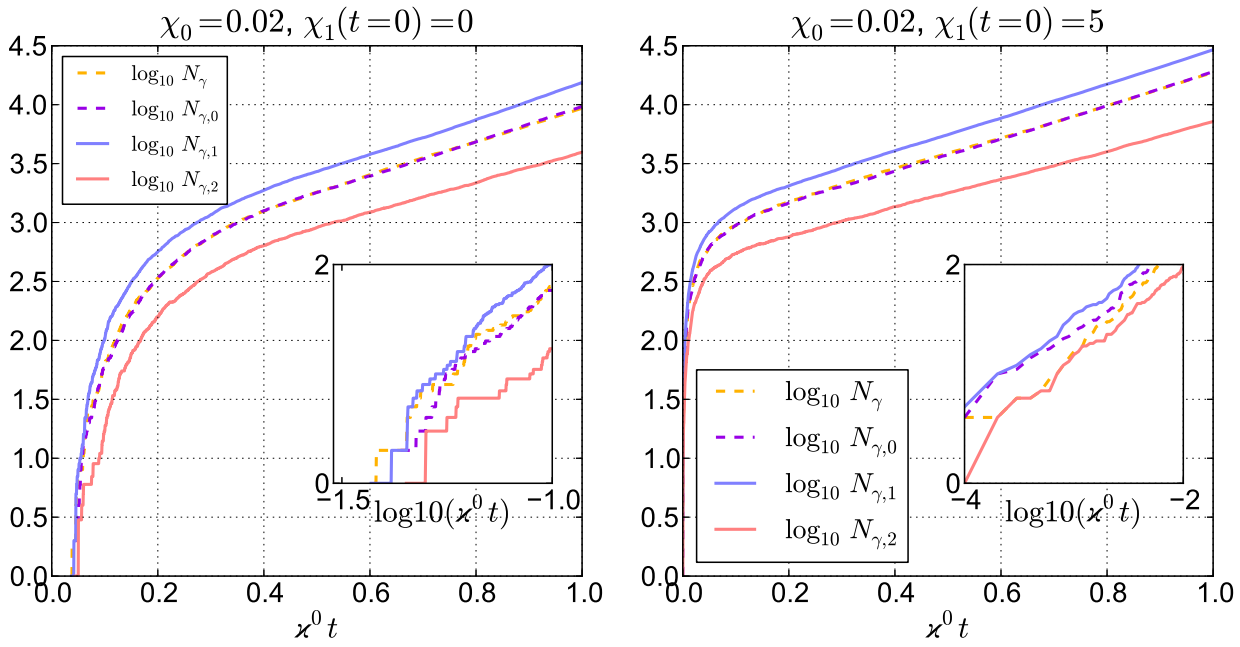

Fig. 7. (Color online). A plot of the logarithm of the number of hard photons ($\chi_k \geq 1$) when 10^3 electrons initially with $\chi_1 = 0, 5$ respectively, interact with a rotating electric field of frequency $\varkappa^0 = 1$ eV, $\xi = 10^4$. In the inset is a log-log plot of the initial stages of the cascade.

0) = 0 case. For the first point, the ratio of $\phi = \pi/2$ to $\phi = 0$ photons can be verified by calculating the ratio of the rates of photon production in each of the two cases. It is not immediately clear that this should be a good approximation as a few generations have been created, whereas the scattering rate is just for the first generation. However, it appears that the single Compton-scattering formula has the good agreement shown in Fig. 10. For the second point, as shown in Figs. 2, 3, taking the unpolarised rate is equivalent to taking the average rate. So the observation that taking a random polarisation of photon or taking the unpolarised rate makes little difference is simply indicative that after thousands of Compton-scattering events, using the average rate for each event is a good approximation. Furthermore, this is supported by noting that N_γ and $N_{\gamma,0}$ are at the average of the positions of $N_{\gamma,1,2}$ just as for the predicted average rate. The final point about the time of onset of Compton scattering being larger for $\chi_1(t=0) = 0$ is also intuitive. As $\chi_1 > 1$ for the other case, Compton scattering can proceed immediately (the time step for the simulation was equivalent to $\varkappa^0 t = 10^{-4}$, which is exactly when pair-creation begins in the right-hand plot of Fig. 7), whereas for $\chi_1(t=0) = 0$, the seed electrons must first be accelerated before

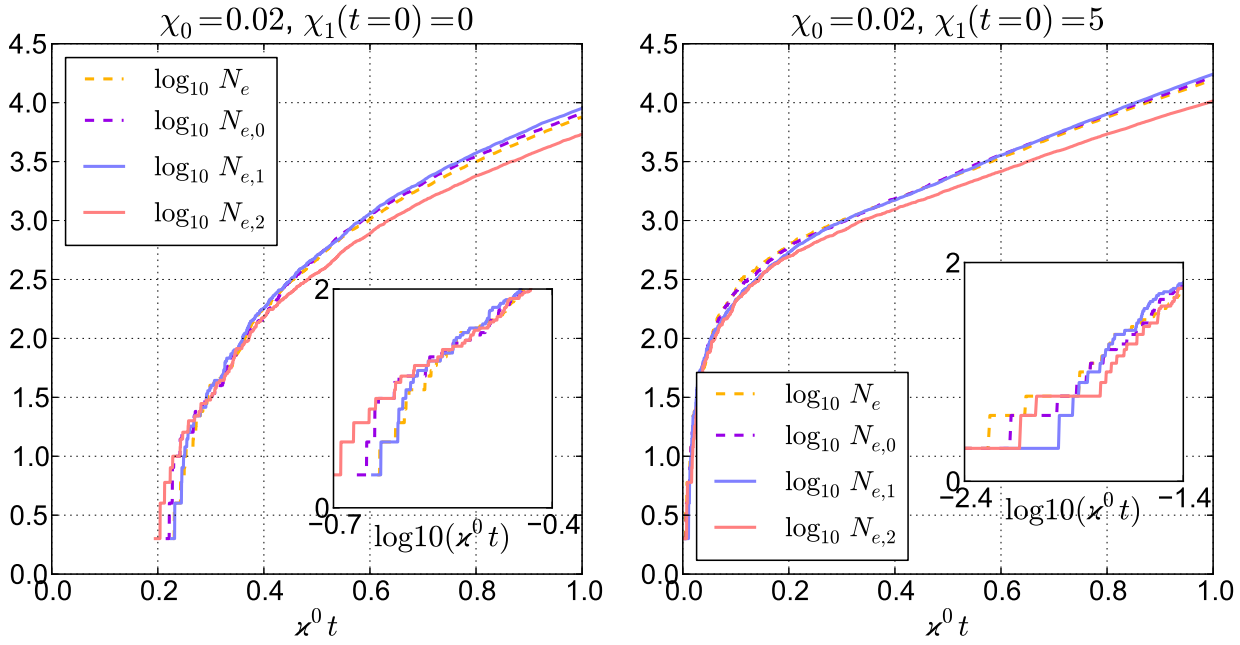

Fig. 8. (Color online). A plot of the logarithm of the number of fermions created in the same set-up as in Fig. 7. When production begins, there is a jump in N_e due to charge conservation (N_e is an even number).

they can produce photons. In a rotating electric field, one can show that the phase required for one of these electrons to reach $\chi_1 = 1$ is $\varkappa^0 t_* = \sqrt{\varkappa^0/m}/\chi_0$ (see [31]). This corresponds to $t_* \approx 0.07$, which is comparable with $t_* \approx 0.05$ from the simulation in Fig. 7.

B. Fermion sector

For the plot of the number of created fermions in Fig. 8, we can make the following observations: i) although the photon-seeded pair-production rate satisfies $R_{e,2} > R_{e,1}$, we notice $N_{e,2} < N_{e,1}$; ii) the difference in the numbers of created pairs using the unpolarised and polarised rate is again small although they are no longer in the middle of the maximum and minimum curves as was the case in the photon sector iii) the time taken for pair-creation to ensue in the electron ensemble initially at ensemble was orders of magnitude larger than for $\chi_1(t = 0) = 5$. The first point can be explained by noting that any pairs created must have gone through a process of N-fold Compton scattering ($N \geq 1$) followed by photon-seeded pair creation. Since pair-production from any low-energy photons created by Compton scat-

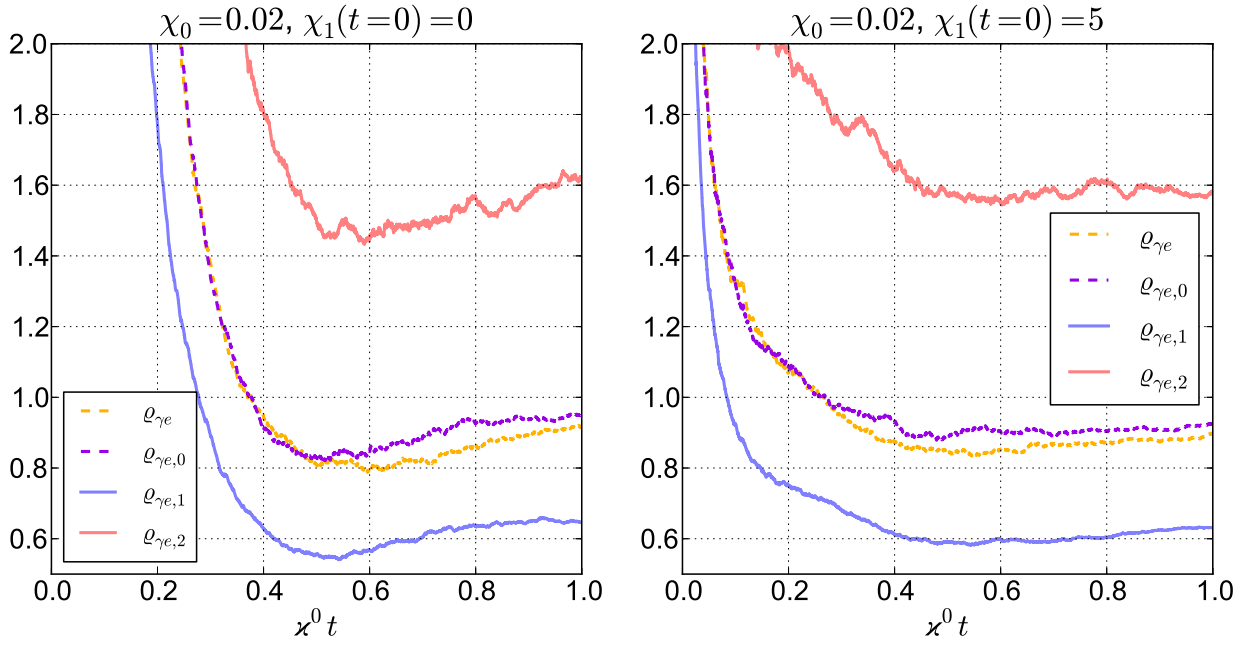

Fig. 9. (Color online). A plot of the ratio of total pairs to created hard ($\chi_k \geq 1$) photons $\varrho_{\gamma e}$. Although pairs are created much earlier in the $\chi_1(t=0)=5$ than in the $\chi_1(t=0)=0$ case, after just $1/2\pi$ periods of the external field, the ratios $\varrho_{\gamma e}$ are already approximately equal.

tering is exponentially suppressed $R_e(\chi_k \ll 1) \sim \chi_k \mathrm{e}^{-8/3\chi_k}/k^0$ [10, 11], we can surmise that only $\chi_k \geq 1$ are relevant on the simulated time scales for pair-creation (in the simulations, a useful approximation was implemented that only $\chi_k \geq 1$ photons were permitted to create pairs). We approximate the ratio of generated pairs from photons polarised with $l = 1, 2$: $\rho_e = N_{e,2}/N_{e,1}$ using the two-step approximation in Eq. (31). This approximation is plotted in Fig. 11 and predicts the correct range of values for around the beginning of the equilibrium period. For larger numbers of Compton-scattered photons, this ratio should be even smaller (the smaller ratio for each Compton-scattering event would likely be amplified), and for larger values of $\varkappa^0 t$, this is also what is observed in the numerics. For point ii), using again the two-step approximation, we note that in the plot of the total rate (Fig. 6), $R_{\gamma e}$ and $R_{\gamma e,0}$ are very close to and even larger than for the maximum polarisation $R_{\gamma e,1}$, for $\chi_1 < 50$ (typical for most fermions in the simulation). This is reflected in both plots in Fig. 11, where the case $\chi_1(t=0)=5$ clearly shows this behaviour for times before equilibrium. The difference between using polarised and unpolarised rates for the two-step process was shown in Fig. 6 to be around 5%. The difference estimated from the pair-creation rate

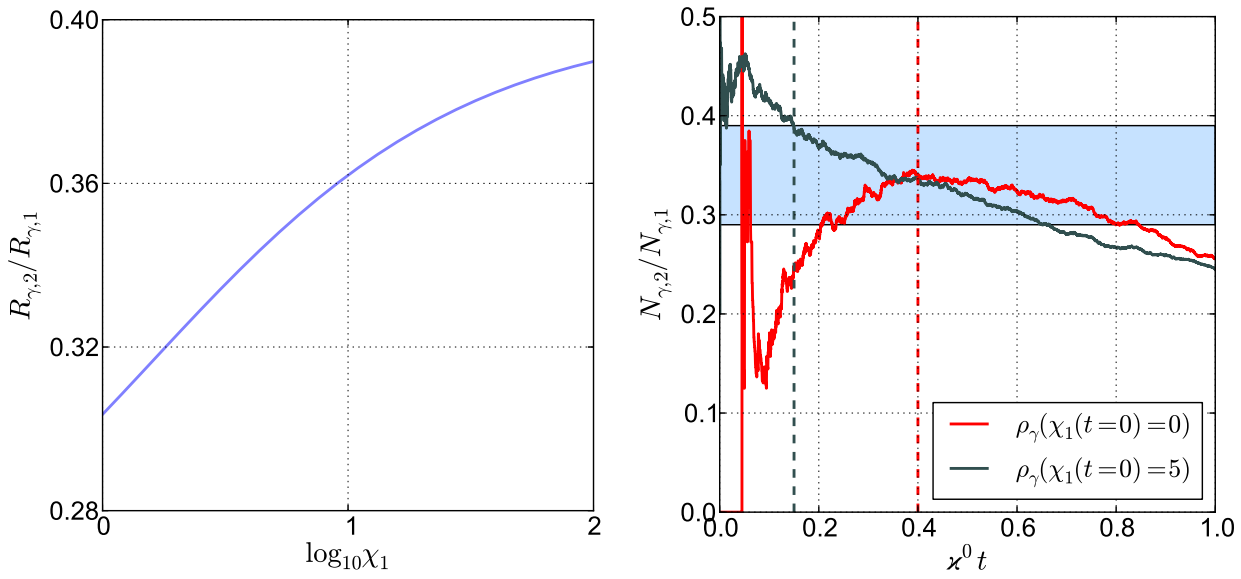

Fig. 10. (Color online). A comparison of the ratio of Compton-scattering rates for the polarisations $\phi = \pi/2, 0$ for a range of χ_1 relevant to the simulation (left-hand plot), with the ratio of numbers of photons generated in the simulation (right-hand plot). The bounds of the shaded region in the latter are given by the left-hand plot, and the vertical dashed lines denote when the "equilibrium" phase of constant exponential growth in Fig. 7 is entered.

for $1 < \chi_1 < 100$ and the estimate of zero for the difference from Compton-scattering are compared to relative yields from simulation $\rho_{\cdot,0} = N_\cdot - N_{\cdot,0}/N_\cdot$ for photons (ρ_γ) and pairs (ρ_e) in Fig. 12 which, taking into account statistical fluctuations, are around the same order of magnitude.

C. Discussion

The results of numerical simulation in the current section and theoretical analysis of Secs. II–IV are in broad agreement. Moreover, the numbers of particles created when polarised tree-level rates were used agreed to within 5% of when unpolarised tree-level rates were used. This was in line with theoretical predictions from Sec. IV for the two-step electron-/positron- seeded pair-creation process when the polarisation of the intermediate photon was averaged over. One can surmise that the large number of seeds in the simulation aided this polarisation averaging effect, which would be reduced when the number of events is small. It was also shown that the number of photons generated with polarisation Λ_1 could be much

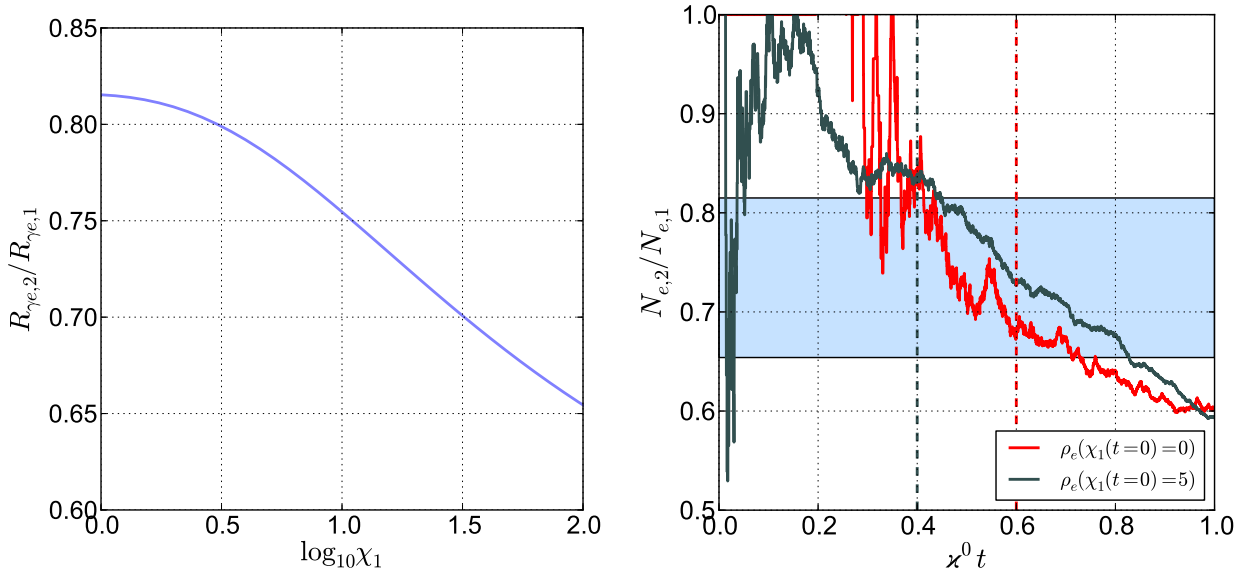

Fig. 11. (Color online). A comparison of the ratio of Compton-scattering rates for the polarisations $\phi = \pi/2, 0$ and a range of χ_1 found in the simulation (left-hand plot), with the ratio of numbers of photons generated in the simulation (right-hand plot), where the bounds of the shaded region are given by the left-hand plot, and the vertical dashed lines denote when the "equilibrium" phase of constant exponential growth in Fig. 7 is entered.

larger than with polarisation Λ_2 and that this led to a significant difference in the number of pairs created by these two polarisations. To put these results in context, since the photon polarisation is transverse to its wavevector, and since the simulation was carried out well into the equilibrium region where initial seed acceleration was shown to make little difference, one might speculate that the photon wavevectors and hence polarisations are in general isotropic. However, when one takes into account the fact that those photon wavevectors in the negative $\hat{z}$ hemisphere are more likely to be generated as Compton scattering in this direction is more likely, with radiation emitted in the $1/\gamma$ emission cone of a relativistic fermion experiencing bremsstrahlung [32], ($\gamma = (1-(v/c)^2)^{-1/2}$ where v is particle velocity and c is the speed of light in vacuum) (see also e.g. [33]), and that these photons are also more likely to lead to pair-creation, then, broadly speaking, the polarisations $\phi = 0, \pi/2$ correspond to the $(0,1,0,0)$ and $(0,0,1,0)$ directions respectively. The simulations presented then demonstrate the principle that, in a system where an anisotropy in the photon vectors exists (such as non-linear Compton-scattering from highly-relativistic electrons in an external field), polarisation

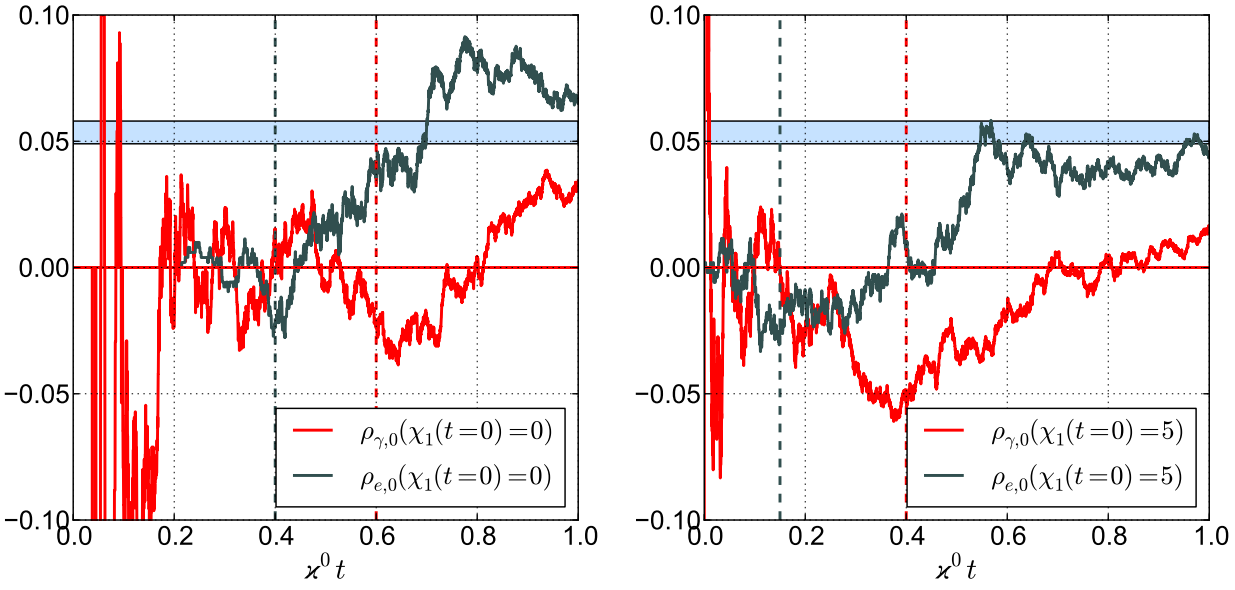

Fig. 12. (Color online). In the plot are the relative differences between the number of photons and pairs produced for the polarised and unpolarised case ($\rho_{\cdot,0} = N_{\cdot} - N_{\cdot,0}/N_{\cdot}$). The solid red horizontal line and grey-blue zones are the predictions using rate arguments for the respective curves.

can play an important role, particularly if this polarisation can be modified by the external field between events in a cascade. It is a straightforward calculation to show that if a photon polarised in the x-y plane with an initial angle ϕ_0 to the x-axis gains a constant phase change $\delta\varphi_{x,y} \ll 1$ along each of these axes, the subsequent rotation angle (dichroism) of the polarisation vector becomes $\delta\phi = -[(\delta\varphi_x - \delta\varphi_y)^2/8]\,\sin 4\phi_0$, and the induced ellipticity is $\varepsilon = [(\delta\varphi_x - \delta\varphi_y)/2]\sin 2\phi_0$. It follows that a randomly-aligned polarisation vector will eventually become either ordinary or extra-ordinary depending on ϕ_0 and remain so (see Fig. 13). Likewise the ellipticity will eventually become zero and the photon linearly-polarised. Although an idealistic model, the simulations presented in the current paper would imply a modification to pair-creation rates in such an environment.

Phase changes can be induced by the polarised vacuum, where it has been shown in more complicated backgrounds such as e.g. focused lasers [34], that $\psi \gg \varepsilon$ is possible, but also in a plasma itself, in which it has been shown that vacuum polarisation effects can also be enhanced [35]. Although likely irrelevant for laser-based experiments as the induced ψ is too small to lead to a significant change in N_γ [34, 36], the polarisation-dependent results

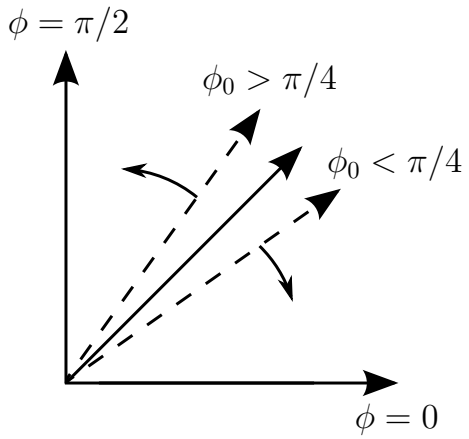

Fig. 13. For a constant phase shift in the x- and y- directions of a photon propagating in the z direction, the diagram represents how the $\phi = \pi/4$ fixed-point is repulsive and the $\phi = 0, \pi/2$ attractive (solid arrows) for initially random photon polarisations (dashed-line arrows). The same behaviour follows in the other quadrant $\pi/2 < \phi < \pi$.

derived in the current paper could be of importance in astrophysical scenarios such as in the field around the magnetospheres of pulsars where $\chi_0 > 0.1$ is possible (one example of this is in the soft gamma-ray repeater SGR 1900+14, [37]). More thorough calculation and modelling of the strong magnetic field is required before the influence of these results in this area can be ascertained.

VI. SUMMARY

We have presented a derivation for the rate of non-linear Compton scattering and photon-seeded pair-creation for linearly-polarised photons in a constant crossed field. Depending on the fixed polarisation of the photon involved, the rates for these processes were seen to vary between $+40\%$ and -80% that of the unpolarised rates. Moreover, those polarisations of photon that were more likely to be produced by non-linear Compton scattering were less likely to be produced by pair-creation and vice versa. To study the combined effect of this disparity, the two-step electron-seeded pair-creation process in a constant crossed field was calculated $e^{\pm} \to e^{\pm} + \gamma$, $\gamma \to e^{+}e^{-}$. Analytical results show that when the photon has a *fixed* polarisation, for incident electron chi-parameter $1 < \chi_1 < 100$ the rate for two-step electron-/positron- seeded pair creation can be up to 30% lower than when the photon is

considered unpolarised. However, the results also show that when the polarisation of the photon is averaged over, the difference from using unpolarised rates for each part of this two-step process, was only around 5%. To test whether photon polarisation plays a role when other chains of Compton-scattering and pair-creation events are involved, for example in the creation of an electron-positron plasma, we used the numerical framework developed in [5, 6]. The results of simulations in a rotating electric field of frequency 1 eV with intensity-parameter $\xi = 10^4$ for the two cases of having 10^3 initial electrons with $\chi_1 = 0$ and $\chi_1 = 5$ were shown to support these conclusions for electromagnetic cascades of on average between two and three generations. On the one hand, the agreement to within 5% in the number of pairs created by using polarised and unpolarised photons was found, supporting this approximation when simulating electron-positron plasmas in intense lasers. On the other, simulations also agreed with another prediction from theory, that the difference between the most and least prevalent photon polarisations was more than 300%, with the difference in the rate of pair-creation from photons with these polarisations being more than 40%. Furthermore, simulations hinted that both these figures grow with time. These results are particularly relevant when the photon vectors are anisotropic and when the photons' polarisation can be modified by its environment.

VII. ACKNOWLEDGEMENTS

B. K. would like to acknowledge useful discussions with P. Böhl. This work was supported by the Grant No. DFG, FOR1048, RU633/1-1, by SFB TR18, projects B12 and B13 and by the Cluster-of-Excellence Munich-Centre for Advanced Photonics (MAP).

[1] N. Bohr and J. A. Wheeler, Phys. Rep. **56**, 426 (1939).

[2] P. M. S. Blackett and G. P. S. Occhialini, Proc. R. Soc. Lond. A **139**, 699 (1933).

[3] W. Heitler, *The quantum theory of radiation (3rd edition)* (Oxford University Press, Amen House, London E. C. 4, 1960).

[4] H. Bethe and W. Heitler, Proc. R. Soc. Lond. A **146**, 83 (1934).

[5] E. N. Nerush et al., Phys. Rev. Lett. **106**, 035001 (2011).

[6] N. V. Elkina et al., Phys. Rev. ST Accel. Beams **14**, 054401 (2011).

[7] C. P. Ridgers et al., Phys. Rev. Lett. **108**, 165006 (2012).

[8] D. L. Burke et al., Phys. Rev. Lett. **79**, 1626 (1997).

[9] H. Chen et al., Phys. Rev. Lett. **102**, 105001 (2009).

[10] L. S. Brown and T. W. B. Kibble, Phys. Rep. **133**, A705 (1964).

[11] A. I. Nikishov and V. I. Ritus, Sov. Phys. JETP **19**, 529 (1964).

[12] K. Krajewska and J. Z. Kamiński, Phys. Rev. A **85**, 062102 (2012).

[13] K. Krajewska and J. Z. Kamiński, Phys. Rev. A **86**, 052104 (2012).

[14] V. I. Ritus, J. Russ. Laser Res. **6**, 497 (1985).

[15] M. Marklund and P. K. Shukla, Rev. Mod. Phys. **78**, 591 (2006).

[16] F. Ehlotzky, K. Krajewska, and J. Z. Kamiński, Rep. Prog. Phys. **72**, 046401 (2009).

[17] A. Di Piazza et al., Rev. Mod. Phys. **84**, 1177 (2012).

[18] C. Thompson and R. C. Duncan, Mon. Not. R. Astron. Soc. **275**, 255 (1995).

[19] A. K. Harding and D. Lai, Rep. Prog. Phys. **69**, 2631 (2006).

[20] T. Heinzl and A. Ilderton, Opt. Commun. **282**, 1879 (2009).

[21] V. Dinu, T. Heinzl, and A. Ilderton, Phys. Rev. D **86**, 085037 (2012).

[22] D. M. Volkov, Z. Phys. **94**, 250 (1935).

[23] V. B. Berestetskii, E. M. Lifshitz, and L. P. Pitaevskii, *Quantum Electrodynamics (second edition)* (Butterworth-Heinemann, Oxford, 1982).

[24] F. W. J. Olver, *Asymptotics and Special Functions* (AKP Classics, A K Peters Ltd., 63 South Avenue, Natick, MA 01760, 1997).

[25] V. N. Baĭer, A. I. Mil'shteĭn, and V. M. Strakhovenko, Sov. Phys. JETP **42**, 961 (1976).

[26] D. E. Aspnes, Phys. Rep. **147**, 554 (1966).

[27] A. Ilderton, Phys. Rev. Lett. **106**, 020404 (2011).

[28] H. Hu, C. Müller, and C. H. Keitel, Phys. Rev. Lett. **105**, 080401 (2010).

[29] S. Meuren and A. Di Piazza, Phys. Rev. Lett. **107**, 260401 (2011).

[30] D. Seipt and B. Kämpfer, Phys. Rev. D **85**, 101701 (2012).

F. Mackenroth and A. Di Piazza, `http://arxiv.org/abs/1208.3424` (2012).

[31] A. M. Fedotov, N. B. Narozhny, G. Mourou, and G. Korn, Phys. Rev. Lett. **105**, 080402 (2010).

[32] J. D. Jackson, *Classical Electrodynamics (3rd Edition)* (John Wiley & Sons, Inc., New York, 1999).

[33] C. Harvey, T. Heinzl, and A. Ilderton, Phys. Rev. A **79**, 063407 (2009).

[34] B. King, A. Di Piazza, and C. H. Keitel, Phys. Rev. A **82**, 032114 (2010).

[35] A. Di Piazza, K. Z. Hatsagortsyan, and C. H. Keitel, Phys. Plasmas **14**, 032102 (2007).

[36] A. Di Piazza, K. Z. Hatsagortsyan, and C. H. Keitel, Phys. Rev. Lett. **97**, 083603 (2006).
T. Heinzl et al., Opt. Commun. **267**, 318 (2006).

[37] C. Kouveliotou et al., Nature **362**, 728 (1993).